A Photoelectronic Switching Device Using a Mixed Self-Assembled Monolayer

Satoshi Nitahara,[†] Tsuyoshi Akiyama,*[,†,‡] Shinobu Inoue,[§] and Sunao Yamada*[,†,‡]

Department of Materials Physics and Chemistry, Graduate School of Engineering, Kyushu University, Hakozaki, Fukuoka 812-8581, Japan, Department of Applied Chemistry, Graduate School of Engineering, Kyushu University, Hakozaki, Fukuoka 812-8581, Japan, and Material Science Laboratory, Mitsui Chemicals, Inc., Nagaura, Sodegaura, Chiba, 299-0265, Japan

Received: July 21, 2004; In Final Form: November 20, 2004

A cathodic−anodic biway photoelectronic device has been successfully constructed using a self-assembled monolayer (SAM). The SAM consists of two kinds of photofunctional thiol derivatives, a ruthenium complex−viologen linked compound (RuVS) and a phthalocyanine derivative (PcS), on a gold electrode. Structural characterization of the SAM has been carried out by absorption spectroscopy, cyclic voltammetry, and differential pulse voltammetry. Photocurrent responses were measured in the presence of methyl viologen (MV^{2+}) and oxygen as electron acceptors and triethanolamine (TEOA) as a sacrificial reagent. For the SAM of RuVS alone, intramolecular electron transfer (ET) was superior to intermolecular ET, resulting in anodic photocurrents even in the presence of MV^{2+} and oxygen at 0 V vs Ag/AgCl. On the contrary, only cathodic photocurrents were observed at 0 V for the SAM of PcS alone. Photocurrents from the mixed SAM of RuVS and PcS were roughly the sum of individual photocurrents from RuVS and PcS. In fact, photocurrents from the mixed SAM of RuVS and PcS were observed in the anodic direction below ∼550 nm, and in the cathodic direction above ∼550 nm at 0 V vs Ag/AgCl. In the case of the mixed SAM of RuS (ruthenium complex disulfide) and PcS, only cathodic photocurrents were observed at 0 V vs Ag/AgCl, due to the lack of an intramolecular ET pathway. The results indicate that in the mixed SAM of RuVS and PcS both dyes can individually function for opposite photocurrent generation. We have also applied the mixed SAM as a photoelectronic logic device by using two LEDs (470 and 640 nm). The system clearly operated as an XOR logic device.

Introduction

A major goal of designing high-performance molecular systems on conductive supports is to build high-density information processing devices or artificial sense organs. To reach this goal, fabrication of molecular wires,[1] molecular switches,[2] molecular logic gates,[3] and photoenergy conversion molecular devices[4] are essentially important. These devices should be miniaturized to the levels of functional molecular sizes for ultimate high-density molecular devices. Thus, self-assembling is one of the most suitable methods to realize high-density molecular devices. Self-assembled monolayers (SAMs) are highly promising for implanting functional molecules on an electrode via sulfur-electrode (gold, indium−tin oxide, and so on) self-assembling, and can exploit the fabrication of individual monomolecular modification on the electrode. Fabrications and evaluations of monomolecular devices between narrow gapped electrodes by using self-assembling have been studied,[5] which confirms the possibility of self-assembling for realizing high-density molecular devices.

Meanwhile, SAMs of electron donor (D)−acceptor (A) pairs on the electrode have attracted great attention for constructing ultrathin film devices with current rectification properties on light irradiation, just like photodiodes, and have been extensively studied for a variety of D−A pairs.[4,6−8] One of the noteworthy advantages of self-assembling is that different molecules can be implanted on the single electrode at once.[6,7,9]

Quite recently, we preliminarily reported, for the first time, a bidirectional photoelectric conversion device using a mixed monolayer assembly of a ruthenium complex−viologen linked thiol derivative (RuVS) and a phthalocyanine thiol derivative (PcS), where the direction (cathodic or anodic) of photocurrents could be controlled by wavelength; thus the system could function as a bidirectional photoelectronic switching device dependent on the irradiation wavelength.[7] This was ascribed to that the photoresponsive molecules individually functioned for photocurrent generation. Later, Matsui et al. also reported a similar bidirectional photoswitching device using stacked polymer nanosheet assemblies.[10] Early studies on a dye-sensitized semiconductor electrode by Bard and co-workers had shown that the direction of dye-sensitized photocurrents depended on the film thickness of dyes, the applied potential, and the semiconductor materials.[11] In those cases, however, the basic principle for photocurrent generation was photoinduced electron transfer between the photoexcited dye and the semiconductor (electrode). Thus, the photocurrent direction was also affected by the band gap of the semiconductor. In our system, on the other hand, intramolecular and intermolecular photoinduced electron transfer between the photoexcited dye and the electron donor (acceptor) molecule is responsible for photocurrent generation. In addition, individual working of two molecular systems immobilized on the same electrode has made it possible to generate a bidirectional photocurrent response dependent on the irradiation wavelength, serving as a photoelectronic XOR logic gate. In this study, we have extensively studied structural characterization and photoelectrochemical properties of the

[†] Department of Materials Physics and Chemistry, Kyushu University.
[‡] Department of Applied Chemistry, Kyushu University.
[§] Mitsui Chemicals, Inc.

10.1021/jp046776u CCC: $30.25
Published on Web 02/15/2005

bidirectional monolayer assembly and have successfully applied the monolayer assembly to a bidirectional photoelectronic switching device.

Experimental Section

Synthetic procedures of a ruthenium complex−viologen linked disulfide [RuVS],[4b] ruthenium complex disulfide [RuS],[4b] and a phthalocyanine disulfide [PcS][12] have been described previously.

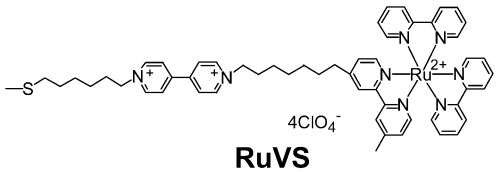

RuVS

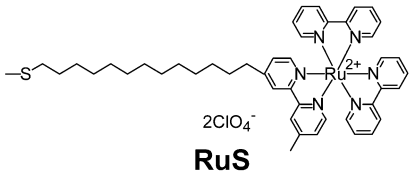

RuS

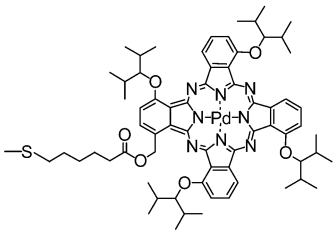

PcS

For the gold electrode, titanium was slightly deposited at first and then gold was deposited on the glass plate by vacuum evaporation.[13] This gold electrode was immersed for 4 days in a mixed solution of CH_3CN and CH_2Cl_2 (1/1 v/v) containing RuVS (1×10^{-3} M). Then the electrode was removed from the solution, rinsed with CH_3CN and CH_2Cl_2, and dried in air to give a modified electrode with RuVS (denoted as RuVS/Au). The modified electrode with PcS, PcS/Au, was also prepared by the same procedure as above. The modified electrode with a mixed monolayer of RuVS and PcS, or RuS and PcS, was also prepared by the same procedures using a mixed solution of a equimolar concentration (1×10^{-3} M) of the corresponding compounds (denoted as (RuVS + PcS)/Au and (RuS + PcS)/Au, respectively).

Cyclic voltammograms (CVs) and differential pulse voltammograms (DPVs) were measured with a Fuso-H1235 potentiostat, by using a three-electrode (photo)electrochemical cell, where the modified (working), Ag/AgCl (sat. KCl) (reference), and platinum (counter) electrodes were used in an aqueous solution of 0.1 M $NaClO_4$ under deaerated condition unless otherwise noted.

Photocurrent measurements on the modified electrodes were carried out using the same three-electrode cell as CV measurements under aerobic condition. In all modified electrodes, methyl viologen (MV^{2+}) as an electron acceptor and triethanolamine (TEOA) as a sacrificial reagent were added in an aqueous 0.1

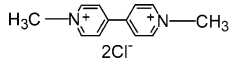

MV^{2+}

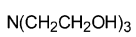

TEOA

M $NaClO_4$ solution. The light from a xenon lamp (300 W) was passed through a monochromator and irradiated the modified electrode of 0.28 cm^2 irradiation area. The photocurrent action spectrum for the modified electrode was measured by changing the excitation wavelength in the 400−750 nm region ($\Delta\lambda = \pm 16$ nm) at selected applied potentials.

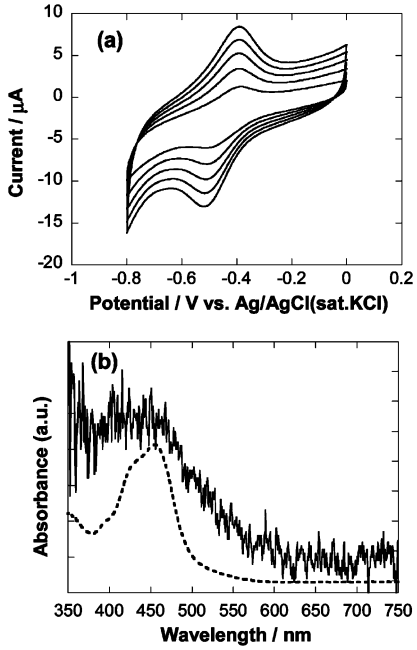

Figure 1. CVs (a) and absorption spectrum (b) of RuVS/Au. In (b), the absorption spectrum of RuVS in acetonitrile (---) is shown.

In the case of logic operation experiments, two kinds of light-emitting diodes (LEDs) were used, where peak wavelengths and average powers were 470 nm and 0.04 W and 640 nm and 0.33 mW, respectively; the former is denoted as LED(blue) and the latter as LED(red). The two LEDs were fixed in front of the photoelectrochemical cell to irradiate the same position of the mixed monolayer assembly, to be able to irradiate simultaneously or independently.

Results and Discussion

In discussing the photocurrent mechanism, information about surface coverages is primarily necessary. The surface coverage of the modified electrode was evaluated by using CV, DPV, and absorption spectroscopy. As shown in Figure 1a, CVs of RuVS/Au showed clear redox waves due to one-electron reduction of the viologen (V^{2+}) moiety (V^{2+}/V^{+}) in the −0.4 to −0.6 V region. This redox couple is a good indication of the immobilization (characterization) of RuVS in the SAM. The peak currents were proportional to the scan rates. By integration of the areas of the reduction waves, the surface coverage of RuVS was evaluated to be 5.5×10^{-11} mol/cm^2. For RuS/Au, no clear redox waves due to the redox of the ruthenium complex moiety were observed in the CV (−1.2 to +1.2 V vs Ag/AgCl). From the molar absorptivity in acetonitrile (1.29×10^4 M^{-1} cm^{-1} at 453 nm) and the absorption spectrum of RuS/Au (Figure 2), the surface coverage was evaluated to be 1.8×10^{-10} mol/cm^2. The surface coverage of RuS was larger than that of RuVS (more than 3 times), probably because the electrostatic repulsion among the RuS was reduced at least to some extent due to the lack of the V^{2+} moiety.

In the case of PcS/Au, no clear redox waves were observed in the CV (−1.0 to +0.8 V vs Ag/AgCl). However, characteristic absorption peaks due to the Q-band of the phthalocyanine moiety were clearly observed for PcS/Au, as shown in Figure

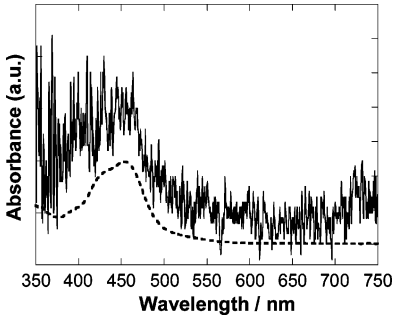

Figure 2. Absorption spectra of RuS/Au (—) and RuS in acetonitrile (---).

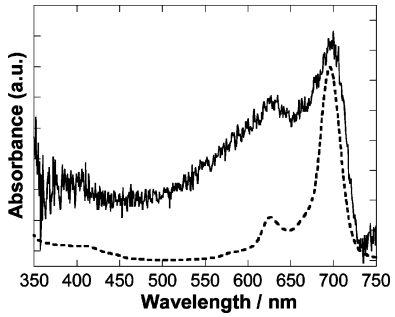

Figure 3. Absorption spectra of PcS/Au (—) and PcS in dichloromethane (---).

3. From the molar absorptivity at 696 nm in dichloromethane (2.5×10^5 M^{-1} cm^{-1}), the surface coverage of PcS was estimated to be 1.6×10^{-11} mol/cm^2.

In the case of mixed SAMs, (RuVS + PcS)/Au and (RuS + PcS)/Au, broad absorption bands in the ~400 to ~500 nm region, characteristic of the metal-to-ligand charge-transfer (MLCT) transition of the ruthenium complex moiety, were essentially overlapped with the absorption spectrum of PcS. Therefore, the evaluation of the surface coverage of RuVS and RuS in the mixed SAMs was difficult from the absorption spectra. Thus, the evaluation of the relative ratio of surface coverage in the mixed SAM was carried out as follows. The gold powder (less than 20 mesh, 0.1 g) was added in the mixed solution of RuVS (or RuS) and PcS (2.0×10^{-6} M each) in $CH_3CN-CH_2Cl_2$ (1:1 v/v) and then the solution was stirred for 70 h, to self-assemble the molecules at the surfaces of gold powder. After stirring ceased, the gold powder precipitated at the bottom of the cell. Thus, the degree of self-assembling can, in principle, be evaluated by measuring the decrease in the absorption intensities of supernatant solution before and after addition of gold powder. Figure 4 shows absorption spectra of the sample solution containing RuVS (or RuS) and PcS (2×10^{-6} M) before and after addition of gold powder and subsequent stirring for 70 h. Molar absorptivities of RuVS, RuS, and PcS at 453 and 696 nm were 1.29×10^4 and 2.20×10^2 M^{-1} cm^{-1} for RuVS and RuS (identical between RuVS and RuS), and 3.64×10^3 and 2.56×10^5 M^{-1} cm^{-1} for PcS, respectively. By using those values and the decrease in the absorbance at 453 and 696 nm, the relative ratios of surface coverages on the gold powder were evaluated to be 3.1:1.0 for RuVS:PcS and 5.0:1.0 for RuS:PcS, respectively. Those ratios were used for evaluating the relative ratio of the surface coverage in the corresponding mixed monolayer assemblies formed on the gold electrodes. Meanwhile, the surface coverage of RuVS in (RuVS + PcS)/Au was evaluated from the reductive wave of the viologen moiety in the CV and DPV (Figure 5). The amount of RuS in (RuS + PcS)/Au was estimated from the as-obtained adsorption ratio of RuS to PcS on the gold

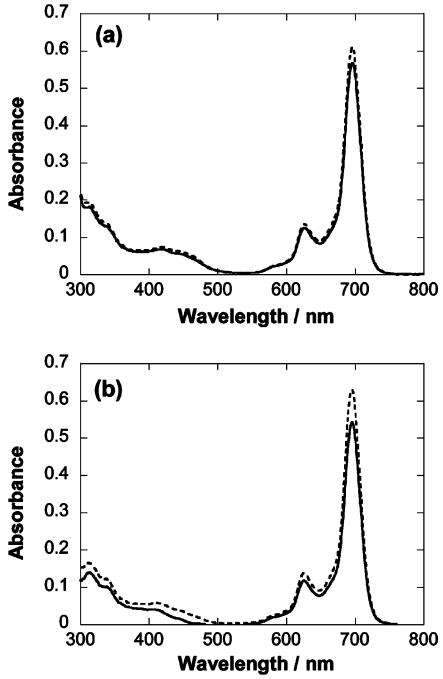

Figure 4. Absorption spectra of sample solution before (---) and after (—) addition of gold powder (0.1 g) in a quartz cell (3 mL) and subsequent stirring for 70 h. Sample solutions: (a) RuVS + PcS (2×10^{-6} M for each); (b) RuS + PcS (2×10^{-6} M for each) in $CH_3CN-CH_2Cl_2$ (1:1 v/v) mixed solvent.

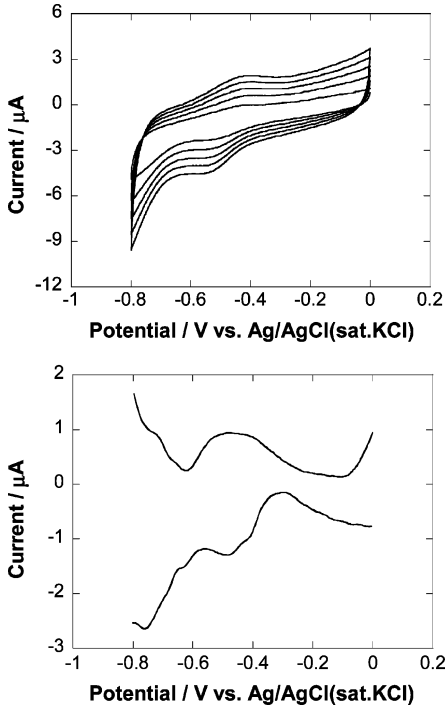

Figure 5. CVs and DPVs of (RuVS + PcS)/Au. Scan rate: 100−500 mV/s. $[NaClO_4] = 0.1$ M.

powder and the absorption spectrum of (RuS + PcS)/Au. These results are summarized in Table 1.

Photocurrent action spectra at 0 V vs Ag/AgCl (sat. KCl) for RuVS/Au and PcS/Au are shown in Figures 6 and 7, respectively. To compare the photocurrent properties with those of other modified electrodes under the identical condition, both MV^{+2} (5×10^{-3} M) and TEOA (5×10^{-2} M) were added in the solution. As shown in Figure 6, the action spectrum of RuVS/Au overlapped well with the corresponding absorption

TABLE 1: Surface Coverages of RuVS, RuS, and PcS in SAMs Formed on the Gold Electrode

compound	surface coverage/$\times 10^{-12}$ mol/cm^2
RuVS	55
RuS	180
PcS	16
RuVS + PcS	6.0,[a] 1.9[b]
RuS + PcS	110,[c] 22[b]

[a] RuVS. [b] PcS. [c] RuS.

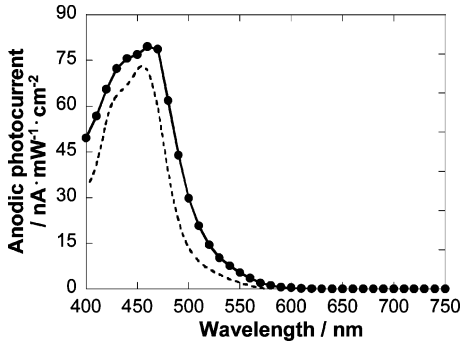

Figure 6. Photocurrent action spectrum of RuVS/Au under aerated condition at $E = 0$ V vs Ag/AgCl (sat. KCl) and absorption spectrum of RuVS in acetonitrile. Conditions: $\Delta\lambda = \pm 16$ nm; [TEOA] $= 5 \times 10^{-2}$ M; [MV^{2+}] $= 5 \times 10^{-3}$ M; [NaClO$_4$] $= 0.1$ M.

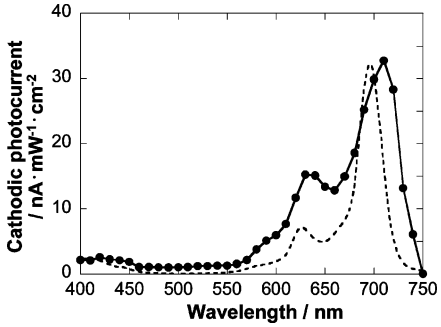

Figure 7. Photocurrent action spectrum of PcS/Au under aerated condition at $E = 0$ V vs Ag/AgCl (sat. KCl) and absorption spectrum of PcS dichloromethane. Conditions: $\Delta\lambda = \pm 16$ nm; [TEOA] $= 5 \times 10^{-2}$ M; [MV^{2+}] $= 5 \times 10^{-3}$ M; [NaClO$_4$] $= 0.1$ M.

spectrum in solution. The anodic photocurrent was somewhat larger (~1.2 times) in the absence of MV^{2+} in the bulk. In addition, deaeration induced little change of the photocurrent intensity. These results clearly show that there is some contribution of intermolecular ET from the photoexcited Ru^{2+} (*Ru) to MV^{2+} in the bulk, which must be responsible for cathodic photocurrent generation. However, it can be concluded that the photocurrent is certainly observed in the anodic direction and thus is ascribed exclusively to intramolecular ET from *Ru to the viologen moiety in RuVS/Au, as has been verified from similar linked systems.[14]

In the case of PcS/Au, the action spectrum also overlapped well with the corresponding absorption spectrum in solution (Figure 7); a slight red shift of the action and absorption peaks is not clear at this stage. Addition of MV^{2+} (5×10^{-3} M) somewhat increased the photocurrent (~5%) under the aerated condition. Different from RuVS/Au, deaeration induced a remarkable reduction of photocurrent (~80%). Thus, oxygen acts as a more efficient electron acceptor for the photoexcited phthalocyanine (Pc) moiety (*Pc) than MV^{2+}. In fact, the photocurrent became substantially smaller (~40%) by the addition of TEOA (5×10^{-2} M) under the aerated condition. Accordingly, the cathodic photocurrent on PcS/Au is mainly

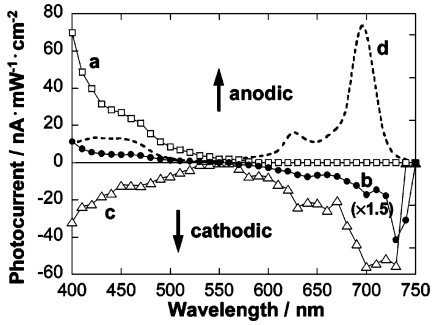

Figure 8. Photocurrent action spectra of (RuVS + PcS)/Au under aerated condition at some applied potentials: (a) +0.4, (b) 0, and (c) −0.2 V vs Ag/AgCl (sat. KCl). The action spectrum (b) is 1.5 times magnified. Conditions: $\Delta\lambda = \pm 16$ nm; [TEOA] $= 5 \times 10^{-2}$ M; [MV^{2+}] $= 5 \times 10^{-3}$ M; [NaClO$_4$] $= 0.1$ M. The absorption spectrum of RuVS + PcS (molar ratio 3.1:1.0) is shown by the dashed line (---) in (d).

attributed to the combination of photoinduced intermolecular ET from *Pc to oxygen and some extent to MV^{2+}, and the concomitant ET from the electrode to *Pc.

Photocurrent action spectra of (RuVS + PcS)/Au at some applied potentials under aerated condition are shown in Figure 8. At $E = -0.2$ V, the spectrum showed broad peaks around ~630 to ~730 nm and the contribution from RuVS was negligible. In the case of $E = +0.4$ V, on the other hand, the photocurrent was observed only in the anodic direction with relatively large peaks around 420−470 nm, and thus the contribution from PcS was considerably small. The results show that RuVS preferentially functions for the anodic photocurrent at $E = -0.2$ V, while PcS does for the cathodic photocurrent at $E = +0.4$ V. The spectrum at $E = 0$ V is also shown in Figure 8b. Note that the spectrum showed a broad anodic peak around 450 nm corresponding to the absorption band of RuVS, and broad cathodic peaks in the ~630 to ~730 nm region corresponding to the absorption peaks of PcS, with a crossing point (zero current) around 550 nm. It is not apparent at this stage why the spectral feature of the action spectrum is somewhat different (red shifted) from the corresponding absorption spectrum. However, there is no doubt that the photocurrent measured in the wavelength region longer than ~600 nm is ascribed from the photoexcitation of PcS alone.

The above photocurrent results indicate that two kinds of photoinduced ET pathways work almost individually in the (RuVS + PcS)/Au as schematically shown in Figure 9. That is, intramolecular photoinduced ET from *Ru^{2+} to V^{2+} in RuVS is mostly responsible for the anodic photocurrents in the shorter wavelength region and the electron was supplied from TEOA to the oxidized ruthenium complex moiety (Ru^{3+}). The contribution of intermolecular ET from *Ru^{2+} to MV^{2+} is substantially smaller. The intermolecular photoinduced ET from *Pc to MV^{2+} and residual oxygen in the bulk is mostly responsible for the cathodic photocurrents observed in the longer wavelength region (Figure 8b).

In any case, one of these two pathways can be preferentially driven by choosing the irradiation wavelength, because the absorption bands of Ru^{2+} (around 450 nm) and Pc (around 600−730 nm) are widely separated from each other. At negative potentials, ET from the electrode to Pc^+ easily occurs in PcS ($E_{ox} = +0.84$ V vs Ag/AgCl), while that from V^{2+} to the electrode becomes difficult in RuVS ($E_{red} = -0.39$ V vs Ag/AgCl). At positive potentials, ET from V^+ to the electrode becomes favorable in RuVS, while that from the electrode to Pc^+ becomes unfavorable. Accordingly, the direction of pho-

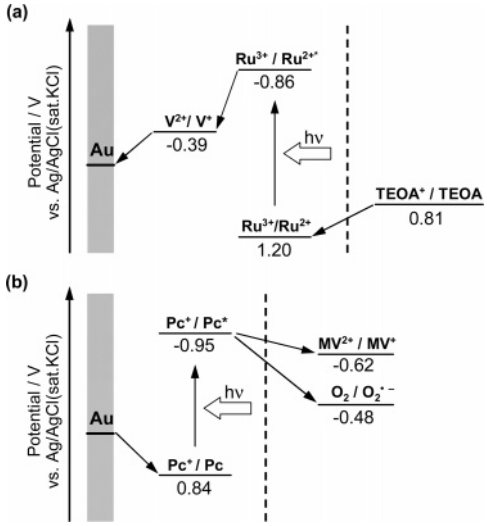

Figure 9. Photocurrent generation diagrams including pathways of electron flow for RuVS/Au (a) and PcS/Au (b). Values denoted below the redox couples are corresponding redox potentials (volts vs Ag/AgCl (sat. KCl)).

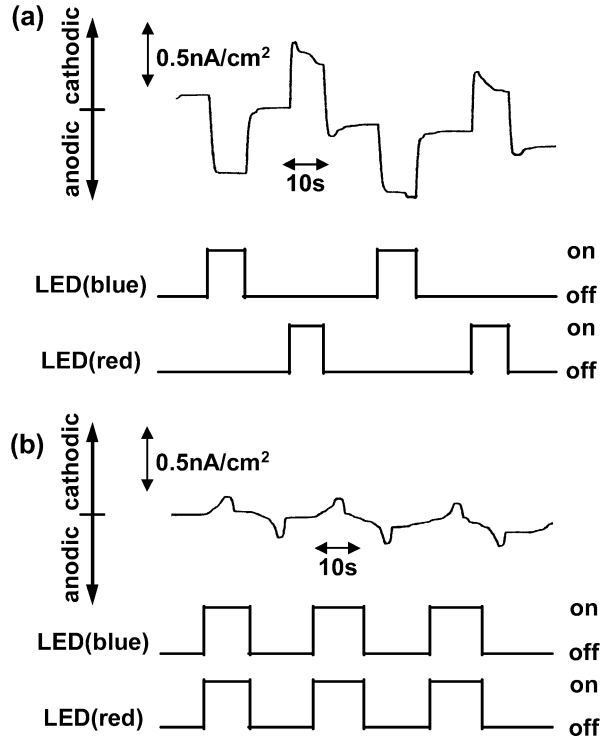

Figure 10. Photocurrent responses from (RuVS + PcS)/Au using LEDs, where LED(blue) and LED(red) are irradiated alternately (a) or simultaneously (b).

tocurrent in (RuVS + PcS)/Au could be controlled by choosing the irradiation wavelength at 0 V vs Ag/AgCl (sat. KCl).

Figure 10 shows photocurrent responses from (RuVS + PcS)/Au, where the two LEDs were used independently (Figure 10a) or simultaneously (Figure 10b). When the mixed monolayer assembly was irradiated by the LED(blue), the anodic photocurrent was observed. On the other hand, the cathodic photocurrent was observed in the case of irradiation by the LED(red). The powers of the LEDs were adjusted to generate almost the same absolute values of the cathodic and anodic photocurrents between the two LEDs. Thus, the mixed monolayer assembly can function as an oppositely operating photodiode array with the different wavelengths. We have also irradiated the mixed monolayer assembly by the two LEDs simultaneously. As shown in Figure 10b, the photocurrent responses were substantially smaller than those irradiated individually (Figure 10a). If the powers of LEDs were adjusted more precisely, the cathodic and the anodic photocurrents would be completely canceled, giving no photocurrent responses. Although the photocurrent was not canceled out completely, such a discrepancy in the photocurrent intensities (Figure 10a,b) is satisfactory to differentiate "0" and "1" in the logic device.

The success of the present study is due to a smart implantation of a couple of individually functioning photoinduced ET systems on the electrode. This novel photocurrent behavior must have promising applications for future molecular photonic devices.

Acknowledgment. The present study was partially supported by a Grant-in-Aid for the 21st Century COE Program, "Functional Innovation of Molecular Informatics", and by a Grant-in-Aid for Scientific Research on Priority Areas (417) and for scientific research (No. 15350085), from the Ministry of Education, Culture, Sports, Science, and Technology of Japan (MEXT). The authors would like to thank Mr. H. Horiuchi for the fabrication of the photoelectrochemical cell, and Mr. Y. Nitahara for designing the LED illumination apparatus.

References and Notes

(1) (a) Bumm, L. A.; Arnold, J. J.; Cygan, M. T.; Dunbar, T. D.; Burgin, T. P.; Jones, L.; Allara, D. L.; Tour, J. M.; Weiss, P. S. *Science* **1996**, *271*, 1705. (b) Tsivgoulis, G. M.; Lehn, J.-M. *Adv. Mater.* **1997**, *9*, 39. (c) Weiss, E. A.; Ahrens, M. J.; Sinks, L. E.; Gusev, A. V.; Ratner, M. A.; Wasielewski, M. R. *J. Am. Chem. Soc.* **2004**, *126*, 5577.

(2) (a) Collier, C. P.; Mattersteig, G.; Wong, E. W.; Luo, Y.; Beverly, K.; Sampaio, J.; Raymo, F. M.; Stoddart, J. F.; Heath, J. R. *Science* **2000**, *289*, 1172. (b) Emberly, E. G.; Kirczenow, G. *Phys. Rev. Lett.* **2003**, *91*, 188301-1. (c) Diehl, M. R.; Steuerman, D. W.; Tseng, H.-R.; Vignon, S. A.; Star, A.; Celestre, P. C.; Stoddart, J. F.; Heath, J. R. *ChemPhysChem* **2003**, *4*, 1335. (d) Zhang, C.; Du, M.-H.; Cheng, H.-P.; Zhang, X.-G.; Roitberg, A. E.; Krause, J. L. *Phys. Rev. Lett.* **2004**, *92*, 158301-1.

(3) (a) Credi, A.; Balzani, V.; Langford, S. J.; Stoddart, J. F. *J. Am. Chem. Soc.* **1997**, *119*, 2679. (b) Lukas, A. S.; Bushard, P. J.; Wasielewski, M. R. *J. Am. Chem. Soc.* **2001**, *123*, 2440. (c) Matsui, J.; Mitsuishi, M.; Aoki, A.; Miyashita, T. *Angew. Chem., Int. Ed.* **2003**, *42*, 2272. (d) de Silva, A.; McClenaghan, N. D. *Chem.—Eur. J.* **2004**, *10*, 574.

(4) (a) Uosaki, K.; Kondo, T.; Zhang, X.-Q.; Yanagida, M. *J. Am. Chem. Soc.* **1997**, *119*, 8367. (b) Terasaki, N.; Akiyama, T.; Yamada, S. *Langmuir* **2002**, *18*, 8666. (c) Yamada, H.; Imahori, H.; Nishimura, Y.; Yamazaki, I.; Ahn, T. K.; Kim, S. K.; Kim, D.; Fukuzumi, S. *J. Am. Chem. Soc.* **2003**, *125*, 9129.

(5) (a) Samanta, M. P.; Tian, W.; Datta, S.; Henderson, J. I.; Kubiak, C. P. *Phys. Rev. B* **1996**, *53*, R7626. (b) Sakaguchi, H.; Hirai, A.; Iwata, F.; Sasaki, A.; Nagamura, T.; Kawata, E.; Nakabayashi, S. *Appl. Phys. Lett.* **2001**, *79*, 3708. (c) Wakamatsu, S.; Akiba, U.; Fujihira, M. *Jpn. J. Appl. Phys.* **2002**, *41*, 4998.

(6) Yamada, S.; Kohrogi, H.; Matsuo, T. *Chem. Lett.* **1995**, 639.

(7) Akiyama, T.; Nitahara, S.; Inoue, S.; Yamada, S. *Photochem. Photobiol. Sci.* **2004**, *3*, 26.

(8) Yamada, H.; Imahori, H.; Nishimura, Y.; Yamazaki, I.; Fukuzumi, S. *Adv. Mater.* **2002**, *14*, 892.

(9) (a) Bain, C. D.; Whitesides, G. M. *Science* **1988**, *240*, 62. (b) Bain, C. D.; Whitesides, G. M. *J. Am. Chem. Soc.* **1988**, *110*, 3665. (c) Bain, C. D.; Whitesides, G. M. *J. Am. Chem. Soc.* **1988**, *110*, 6560.

(10) Matsui, J.; Mitsuishi, M.; Aoki, A.; Miyashita, T. *J. Am. Chem. Soc.* **2004**, *126*, 3708.

(11) (a) Jaeger, C. D.; Fan, F.-R. F.; Bard, A. J. *J. Am. Chem. Soc.* **1980**, *102*, 2592. (b) Giraudeau, A.; Fan, F.-R. F.; Bard, A. J. *J. Am. Chem. Soc.* **1980**, *102*, 5137.

(12) Yamada, S.; Akiyama, T.; Inoue, S.; Misawa, T. Jpn. Pat. 2003-123863, 2003

(13) Naohara, H.; Ye, S.; Uosaki, K. *Colloids Surf., A* **1999**, *154*, 201.

(14) Koide, Y.; Terasaki, N.; Akiyama, T.; Yamada, S. *Thin Solid Films* **1999**, *350*, 223.